



Can seasonal and interannual variation in landscape CO₂ fluxes be detected by atmospheric observations of CO₂ concentrations made at a tall tower?

T. L. Smallman^{1,2}, M. Williams^{1,2}, and J. B. Moncrieff¹

¹School of GeoSciences, University of Edinburgh, Edinburgh, EH9 3JN, UK

²National Centre for Earth Observation, University of Edinburgh, Edinburgh, EH9 3JN, UK

Correspondence to: T. L. Smallman (t.l.smallman@ed.ac.uk)

Received: 17 July 2013 – Published in Biogeosciences Discuss.: 27 August 2013

Revised: 16 December 2013 – Accepted: 31 December 2013 – Published: 6 February 2014

Abstract. The coupled numerical weather model WRF-SPA (Weather Research and Forecasting model and Soil-Plant-Atmosphere model) has been used to investigate a 3 yr time series of observed atmospheric CO₂ concentrations from a tall tower in Scotland, UK. Ecosystem-specific tracers of net CO₂ uptake and net CO₂ release were used to investigate the contributions to the tower signal of key land covers within its footprint, and how contributions varied at seasonal and interannual timescales. In addition, WRF-SPA simulated atmospheric CO₂ concentrations were compared with two coarse global inversion models, CarbonTrackerEurope and the National Oceanic and Atmospheric Administration's CarbonTracker (CTE-CT). WRF-SPA realistically modelled both seasonal (except post harvest) and daily cycles seen in observed atmospheric CO₂ at the tall tower ($R^2 = 0.67$, $\text{rmse} = 3.5$ ppm, $\text{bias} = 0.58$ ppm). Atmospheric CO₂ concentrations from the tall tower were well simulated by CTE-CT, but the inverse model showed a poorer representation of diurnal variation and simulated a larger bias from observations (up to 1.9 ppm) at seasonal timescales, compared to the forward modelling of WRF-SPA. However, we have highlighted a consistent post-harvest increase in the seasonal bias between WRF-SPA and observations. Ecosystem-specific tracers of CO₂ exchange indicate that the increased bias is potentially due to the representation of agricultural processes within SPA and/or biases in land cover maps. The ecosystem-specific tracers also indicate that the majority of seasonal variation in CO₂ uptake for Scotland's dominant ecosystems (forests, cropland and managed grassland) is detectable in observations within the footprint of the tall tower; however, the amount of variation explained varies between

years. The between years variation in detectability of Scotland's ecosystems is potentially due to seasonal and interannual variation in the simulated prevailing wind direction. This result highlights the importance of accurately representing atmospheric transport used within atmospheric inversion models used to estimate terrestrial source/sink distribution and magnitude.

1 Introduction

The global climate is changing and these changes are driven by human activities, in particular by anthropogenic emissions of CO₂ (IPCC, 2007). The terrestrial biosphere currently absorbs a significant fraction of anthropogenic emissions of CO₂ (Canadell et al., 2007). However, terrestrial ecosystems are highly complex and dynamic, creating a net land–atmosphere surface exchange that can be either a source or sink of CO₂. Furthermore, the magnitude of sources and sinks vary both spatially and temporally, resulting in significant seasonal, interannual and spatial variation. The magnitude of net ecosystem exchange of CO₂ (NEE) is significantly impacted by changes in weather, climate and human management, adding further complexity to ecosystem processes (IPCC, 2007). Higher spatial and temporal resolution observations over multi-annual periods are required to detect fine scale ecosystem heterogeneity and ecosystem response to drivers. A critical objective is an improved understanding of the information contained within observations of atmospheric greenhouse gas concentrations.

Both forward running and atmospheric inversion models have been used in conjunction with observations of atmospheric CO₂ concentrations to investigate regional scale exchange of CO₂. Forward running models, such as WRF (Weather Research and Forecasting model) or RAMS (Regional Atmospheric Modeling System), have been used to investigate a wide range of topics, including the impact of surface processes on atmospheric transport (e.g. Steeneveld et al., 2011) and how ecosystems contribute to observations made at the regional scale (e.g. Tolk et al., 2009). Inverse atmospheric models, which infer surface fluxes from measurements of atmospheric CO₂ concentrations (e.g. made at a tall tower), have been used to constrain the terrestrial carbon balance at global, continental and regional scales (Gurney et al., 2002; Peters et al., 2010; Lauvaux et al., 2012). Inverse models are able to detect large-scale, large magnitude interannual variations in CO₂ exchange. For example, the Europe-wide heat wave in 2003 has been linked to a large-scale reduction in carbon sequestration across Europe (Ciais et al., 2005; Peters et al., 2010). However, there remains uncertainty over the ability of regional scale inversions to successfully quantify small magnitude changes in surface fluxes. Peters et al. (2010) suggested two contrasting hypotheses to explain increases in regional estimates of sequestration in the years following the European 2003 heat wave. First, increased sequestration may have been due to interannual variation in plant phenology. Second, changes to atmospheric transport due to interannual variation in weather (e.g. due to turbulent exchange) may have significantly altered the footprint of tall tower observations.

Observations of atmospheric CO₂ concentrations made at tall towers contain seasonal and interannual phenological information about ecosystems near the tower (Miles et al., 2012). However, the correlation between surface NEE and observed profiles of atmospheric CO₂ concentration declines with increasing distance from the observation tower (Gerbig et al., 2009; Miles et al., 2012). A reduction in correlation between tall tower observations and ecosystem activity is consistent with signal dilution due to atmospheric transport (Gerbig et al., 2009; Miles et al., 2012). The dominant influence on observations of atmospheric CO₂ concentrations are from the near field, although the total footprint can cover a large area. For example, an area of $\sim 500 \text{ km} \times 700 \text{ km}$ has been simulated to contribute up to $\sim 50\%$ of the observed signal at the Cabauw tall tower in the Netherlands, while the land surface at the edge of this area contributes ~ 10 times less than the land surface directly beneath the Cabauw tower (Vermeulen et al., 2011). Similarly, Gerbig et al. (2009) investigated the Harvard Forest tower, USA, estimating that the land surface fluxes within 20–60 km of the tower contributed a similar amount to observations as all other areas within their simulated domain combined (5000 km \times 5000 km). Furthermore, atmospheric inversions are unable to attribute variations and/or anomalies in atmospheric CO₂ concentrations to a specific ecosystem process

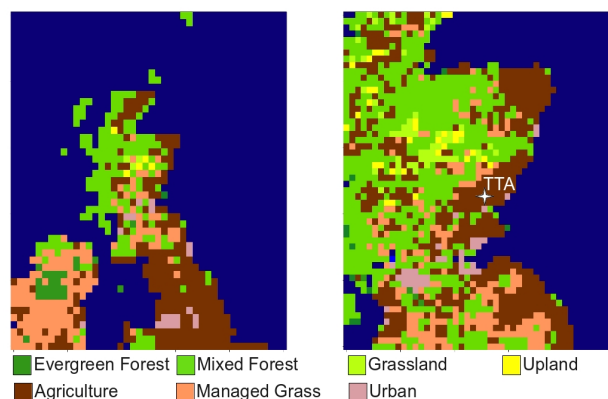


Fig. 1. Land classification map used covering the spatial extent of the model domain. The left panel is the parent domain at $18 \times 18 \text{ km}$, right panel is nested domain at $6 \times 6 \text{ km}$. The star indicates the location of tall tower Angus. The map used in WRF-SPA is a modified MODIS land cover map provided with the WRF model. The fractions of each land cover within the nested domain are crop 36 %, evergreen forest 1 %, mixed forest 42 %, grassland 2 %, managed grassland 13 %, upland 3 %, urban 3 %.

(e.g. respiration or photosynthesis). A forward model has the advantage that processes and source area contributing to the atmospheric CO₂ signal can be directly investigated.

We used a mesoscale model, WRF-SPA (Weather Research and Forecasting model coupled with Soil-Plant-Atmosphere model), operating in forward mode to simulate a 3 yr period between 2006 and 2008 over northern Britain (Fig. 1), which includes Scotland, the geographical focus of this paper. Simulated atmospheric CO₂ concentrations from WRF-SPA and a global atmospheric inversion model were compared to observations made at tall tower Angus (TTA) on the east coast of Scotland. TTA is currently Scotland's only tall tower equipped for measurement of atmospheric CO₂ concentrations. WRF-SPA provides a means to upscale land surface exchanges, such as photosynthesis and respiration, using atmospheric CO₂ tracers, to observations made mostly within the planetary boundary layer (PBL) of regionally integrated CO₂ concentrations, i.e. those made at TTA.

The overall aim of this paper is to use ecosystem-specific CO₂ tracers of net uptake and net release of CO₂ to improve our understanding of how different ecosystems contribute to observations of atmospheric CO₂ concentrations and relate these contributions to surface processes (Tolk et al., 2009). A unique aspect of this study is the 3 yr observation data set used to consider the detection of both seasonal and interannual variation.

Here we address the following questions:

- i. Does WRF-SPA more accurately simulated observed atmospheric CO₂ concentrations compared to a coarse resolution global atmospheric inversion model?

- ii. Can ecosystem-specific CO₂ tracers be used to inform on which ecosystem processes and land covers are responsible for observed variations in atmospheric CO₂ concentrations?
- iii. Can observations made at TTA detect variation in ecosystem carbon uptake, for ecosystems within the footprint of TTA, at seasonal and interannual timescales?

2 Model description: WRF-SPA

WRF-SPA (Smallman et al., 2013) is a coupling between the high resolution non-hydrostatic mesoscale model Weather Research and Forecasting (WRF) and the mechanistic land surface model (LSM) Soil-Plant-Atmosphere (SPA). SPA is fully integrated into the WRF model framework, where WRF simulates meteorological fields and atmospheric transport of the CO₂ fields. SPA in return provides WRF with surface temperature, roughness length, albedo, and exchanges of energy, heat, water and CO₂. A brief description of the WRF and SPA models are given below.

2.1 WRF

The Weather Research & Forecasting model (WRFv3.2) (<http://www.mmm.ucar.edu/wrf/users/>, accessed 19 October 2009, 15:00 UTC) is a state-of-the-art non-hydrostatic mesoscale meteorological community model (Skamarock et al., 2008). WRF provides a highly adaptable model framework into which SPA has been integrated. In addition to simulating meteorology, WRF is responsible for simulating atmospheric transport of CO₂ tracers released by SPA and originating from the anthropogenic and oceanic flux maps as well as lateral boundary and initial conditions. WRFv3.2 includes a number of land surface maps that include vegetation type and soil classification used by SPA and also orography, which impacts simulation of air flow within the model (Mesoscale and Microscale Meteorology Division, 2011).

2.2 SPA

The SPA model is a high vertical resolution mechanistic terrestrial ecosystem model (up to 10 canopy layers and 20 soil layers). SPA provides WRF with surface fluxes of heat, water and CO₂ exchange in response to meteorological drivers through a close coupling of its hydrological and carbon cycles, based on eco-physiological principles (Williams et al., 1996). Detailed descriptions of the major SPA developments can be found in Williams et al. (1996, 1998, 2001, 2005), Sus et al. (2010) and Smallman et al. (2013).

WRF provides SPA with meteorological drivers, including air temperature, precipitation, vapour pressure deficit (VPD), wind speed, friction velocity, atmospheric CO₂ mixing ratios, air pressure, and short- and long-wave incoming

radiation. SPA currently has parameters for 8 vegetation types (evergreen forest, deciduous forest, mixed forest, arable cropland, managed grassland, grassland, upland and urban) suitable for UK application and 13 soil types impacting soil hydrology. Vegetation cover is specified by the MODIS land cover map provided with WRFv3.2, while soil classifications are from the default WRF soil cover maps (Mesoscale and Microscale Meteorology Division, 2011).

The Farquhar model of photosynthesis (Farquhar and von Caemmerer, 1982), the Penman–Monteith model of leaf transpiration (Jones, 1992) and the leaf energy balance are coupled via a mechanistic model of stomatal conductance. Stomatal conductance is modelled by linking atmospheric demand for water and available water supply from the soil through plant hydraulics (Williams et al., 1996, 2001). SPA maximises carbon assimilation per unit nitrogen within a minimum leaf water potential constraint to prevent cavitation (Williams et al., 1996). SPA uses detailed multi-layer parameterisations of canopy processes, including radiative transfer (Williams et al., 1998), above and within canopy momentum decay and leaf level boundary layer conductance (Smallman et al., 2013).

Plant phenology is described by a box carbon model to simulate the main ecosystem carbon (C) pools (Williams et al., 2005; Sus et al., 2010). C pools are foliage, structural wood carbon, fine roots, labile, soil organic matter (SOM) and surface litter. Crops have two additional C pools: storage organ C (i.e. harvestable C) and dead foliar C (still standing). The C pools within WRF-SPA are “spun-up”, as described in Smallman et al. (2013), using meteorology, which is broadly representative of the median meteorological conditions in Scotland. The carbon model provides a direct coupling between the plant carbon cycle and plant phenology, specifically foliar and fine root C. Foliar C determines the leaf area index (LAI) while fine root C impacts water uptake potential.

2.3 Initial and lateral boundary conditions for CO₂

Initial conditions (IC) and lateral boundary conditions (LBC) for atmospheric CO₂ (except 2008) are from CarbonTrackerEurope (CTE, Peters et al., 2010) providing 1° × 1° resolution fields at 3-hourly update intervals. Optimised CO₂ fields were not available for 2008 from CTE; instead, CO₂ fields for 2008 are from CarbonTracker (Peters et al., 2007). These are also available at 3-hourly update intervals, but at a coarse 3° × 2° resolution. IC and LBC for atmospheric CO₂ were linearly interpolated to the WRF-SPA domain.

Global flux maps of anthropogenic CO₂ emissions and ocean absorption were used to provide non-biospheric surface CO₂ exchange. The global flux maps were also from CTE at 1° × 1° resolution with 3-hourly update intervals. Fluxes were interpolated using 4 point weighted mean based on latitude and longitude coordinates. Biospheric fluxes of CO₂ are simulated by SPA. All surface CO₂ fluxes were

calculated as rates which were added to the lowest model atmospheric layer in each time step.

2.4 Atmospheric CO₂ tracers

WRF-SPA has been modified with the addition of several atmospheric CO₂ tracer pools (Table 1). CO₂ tracer transport is simulated within the model domain concurrently with meteorological variables; feedback on atmospheric radiative transfer due to variable CO₂ is neglected as its impact is expected to be small.

We compared simulated atmospheric CO₂ with an active biosphere versus simulated without a biosphere (“forcings only”). “Forcings only” CO₂ tracer contains IC, LBC, anthropogenic emissions and ocean sequestration of CO₂ (i.e. CO₂ exchange not calculated by WRF-SPA) but no exchange with the SPA simulated biosphere. Comparison between the total atmospheric CO₂ concentration and “forcings only” CO₂ concentration allows for isolation of the impact due to inclusion of the simulated biosphere. Furthermore, CTE (2006–2007) and CT (2008) atmospheric CO₂ concentrations are compared to TTA observations to assess how well CTE-CT simulates atmospheric CO₂ at a tower not included in the inversion model.

2.4.1 Ecosystem-specific tracers

The ecosystem-specific tracers of net uptake and net release of CO₂ are used to investigate the information content on these processes contained within the total atmospheric CO₂ concentrations simulated at TTA. We investigate how representative observations at TTA are of the underlying surface fluxes of CO₂. Note that LBCs for the outer domain have been set with zero inflow and zero-gradient outflow for ecosystem-specific net uptake and net release CO₂ tracers. Zero gradient inflow/outflow allow tracers to easily leave the domain and prevent artificial influx to the CO₂ tracer fields.

The land surface can be either a net source or net sink of atmospheric CO₂, varying both spatially and temporally. Whether the land surface is a net sink or source of CO₂ is determined by the net result of photosynthetic and respiratory processes. Atmospheric CO₂ concentrations represent a spatial and temporal integration of the net flux of CO₂ between the land surface and the lower atmosphere. Therefore, when the simulated surface flux of CO₂ represents a net removal of CO₂ from the atmosphere, an ecosystem-specific “net uptake CO₂ tracer” is released into the simulated atmosphere at the same rate as the “surface net CO₂ uptake flux” (i.e. rate of NEE). Correspondingly, when the surface net CO₂ uptake flux represents a net addition of CO₂ to the atmosphere, an ecosystem-specific “net release CO₂ tracer” is released.

The net uptake CO₂ tracers are considered to be non-interacting/non-interactive, while the net release CO₂ tracers are interacting/interactive. The net uptake CO₂ tracers are non-interacting as they represent a removal of atmospheric

CO₂ and as such cannot interact with the land surface. After their emission from the surface, the net uptake CO₂ tracers are transported through the model atmosphere. Conversely, net release CO₂ tracers represent an addition of a physical mass of CO₂ to the atmosphere via respiration, which can therefore be subsequently removed from the atmosphere by photosynthesis after its initial release. Allowing the removal of a net release CO₂ tracer prevents a respiratory signal from being simulated at TTA, which in reality does not reach TTA due to being consumed en route in a physically consistent manner.

Net release CO₂ tracers are removed from the atmosphere if they are present in the lowest model atmospheric level and the land surface below represents a net removal of CO₂. If there are multiple ecosystem-specific net release CO₂ tracers present in the same model atmosphere grid box, then removal is determined by the relative fraction of each ecosystem-specific tracer. For example, to determine the removal of crop net release CO₂ tracer,

$$\gamma \uparrow t_{\text{crop}rm} = \frac{\uparrow t_{\text{crop}}}{\uparrow t_{\text{crop}} + \uparrow t_{\text{forest}} + \uparrow t_{\text{grass}} + \uparrow t_{\text{other}}}, \quad (1)$$

where $\gamma \uparrow t_{\text{crop}rm}$ is the fraction of surface CO₂ flux (i.e. NEE) to be applied to the crop net release CO₂ tracer. $\uparrow t_{\text{crop}}$ is the crop net release (arrow indicating direction and t indicating it as a tracer) CO₂ tracer concentration, similarly for forest, managed grassland and “other” land cover types.

2.4.2 Investigating representativeness and detection of seasonal and interannual variation using CO₂ tracers

Ecosystem-specific CO₂ tracers are used to infer representativeness of the simulated atmospheric CO₂ concentrations at TTA of surface CO₂ flux and to investigate how much seasonal and interannual information is contained within these atmospheric CO₂ concentrations. We assumed that the simulated atmospheric CO₂ tracers are driven by the simulated surface CO₂ fluxes (from which they originate) and that atmospheric transport determines how much information on surface fluxes is represented within atmospheric CO₂ concentrations at any given location within the simulated atmosphere. To minimise the effects of short-term transport and to focus only on large seasonal variations, we conducted these analyses using monthly mean values.

We investigated the representativeness of atmospheric CO₂ concentrations simulated at TTA of surface CO₂ flux. We compared the fraction of each ecosystem-specific net uptake CO₂ tracer (e.g. for crop $\downarrow t_{\text{crop}}$) simulated at TTA to the fraction of ecosystem-specific surface net CO₂ uptake flux (e.g. for crop $\downarrow f_{\text{crop}}$, where f indicates this is a flux). Each flux is the integral over the land surface included within the land surface mask detailed in Sect. 3.1.

Table 1. Tracer pools and definitions used by WRF-SPA. A non-interacting tracer does not have the potential to be exchanged with the land surface after its initial emission. An interacting tracer can be removed from the atmosphere as it represents a physical mass of CO₂ added to the atmosphere through respiration.

Tracer	Description	Interacting tracer
1	Total CO ₂ concentration; includes all sources and sinks of CO ₂ for comparison to observations	Yes
2	Forest net CO ₂ uptake	No
3	Anthropogenic emissions	Yes
4	Forcings only, i.e. anthropogenic emissions, ocean sequestration, initial and lateral boundary conditions only	No
5	Crop net CO ₂ uptake	No
6	Ocean sequestration	No
7	Forest net CO ₂ release	Yes
8	Crop net CO ₂ release	Yes
9	Managed grassland net CO ₂ release	Yes
10	Other vegetation net CO ₂ release	Yes
11	Managed grassland net CO ₂ uptake	No
12	Other vegetation net CO ₂ uptake	No

$$\gamma \downarrow t_{\text{crop}} = \frac{\downarrow t_{\text{crop}}}{\downarrow t_{\text{crop}} + \downarrow t_{\text{forest}} + \downarrow t_{\text{grass}} + \downarrow t_{\text{other}}}, \quad (2)$$

$$\gamma \downarrow f_{\text{crop}} = \frac{\downarrow f_{\text{crop}}}{\downarrow f_{\text{crop}} + \downarrow f_{\text{forest}} + \downarrow f_{\text{grass}} + \downarrow f_{\text{other}}}. \quad (3)$$

Representativeness for any given ecosystem type is assumed to be when

$$\gamma \downarrow t_{\text{crop}} \approx \gamma \downarrow f_{\text{crop}}. \quad (4)$$

Moreover, this comparison provides an indication of whether the activity of a given ecosystem is over-represented (i.e. $\gamma \downarrow t_{\text{crop}} > \gamma \downarrow f_{\text{crop}}$) or under-represented (i.e. $\gamma \downarrow t_{\text{crop}} < \gamma \downarrow f_{\text{crop}}$) in simulated atmospheric CO₂ concentrations. Such information can help the interpretation of results from comparing ecosystem-specific CO₂ tracers and the simulated atmospheric CO₂ concentrations.

Investigation of seasonal variation is achieved through linear regression analysis between the surface net CO₂ uptake flux and net uptake CO₂ tracer concentration for a given land cover type. As net uptake CO₂ tracers originate from the simulated surface net CO₂ uptake flux, differences between seasonal variation of tracer concentrations and surface fluxes are due to how atmospheric transport relays variations in flux to TTA. To investigate interannual variation simulated to be detected at TTA, we assume that a change in surface net CO₂ uptake flux for a given ecosystem should be reflected in the net uptake CO₂ tracers simulated at TTA.

2.5 Model domain

The WRF-SPA simulation is comprised of two grids in two-way nesting mode; the outer domain has a resolution of 18 km × 18 km and inner domain has a resolution of 6 km × 6 km (Fig. 1). Scotland provides a highly complex topography and land use heterogeneity, with a longitudinal

gradient from dominantly forested and peatland areas in the northwest to pasture in the central and southwest and arable cropland in the east.

All meteorological data required, e.g. sea surface temperature (SST), soil initialisation, initial conditions and lateral boundary conditions, were taken from the Global Forecasting System (GFS) reanalysis product (<http://www.emc.ncep.noaa.gov/>). GFS data are available at 1° × 1° longitude/latitude resolution with 6-hourly time steps (available from <http://rda.ucar.edu/datasets/ds083.2/>). The main features of the WRF model setup are presented in Table 2.

3 Tall tower observations

Observations of atmospheric CO₂ concentration are from TTA, a 222 m tower (observation height) near Dundee, Scotland (56.56° N, 2.99° W). TTA is equipped for continuous measurement of atmospheric CO₂ concentrations, producing half-hourly observations which have been averaged to hourly timescales for comparison with WRF-SPA. TTA has been operational since the end of 2005 to the current date. Observations made at TTA have an accuracy limit of 0.1 ppm. TTA was part of the CHIOTTO network during the period of analysis reported here (EVK2-CT-2002-00163) and as such was fully integrated into the calibration and validation methodologies of that project. The data continues to be quality controlled under the InGOS project (<http://www.ingos-infrastructure.eu/>, accessed 9 December 2013, 16:30 UTC).

3.1 TTA footprint

Currently there are no published assessment of TTA's observation footprint; however, the footprint of Mace Head, located on the west coast of Ireland, has been assessed in multiple studies (e.g. Henne et al., 2010; Rigby et al., 2011; Brunner et al., 2012). Mace Head is exposed to similar

Table 2. Parameter and model options used in WRF-SPA.

Parameter	WFA-SPA model options
Basic equations	Non-hydrostatic, compressible Advanced Research WRF (ARW)
Radiative transfer scheme	Rapid Radiative Transfer Model for GCMs (RRTMG) for both long-wave and short-wave
Planetary boundary layer scheme	Yonsei University
Surface scheme	Monin–Obukov
Microphysics scheme	WSM 3-class simple ice
Cumulus parameterisation	Grell 3-D ensemble scheme (coarse domain only)
Nesting	Two-way nesting
Model time step	Outer = 90 s, inner = 30 s
Domain, resolution	44 × 47, 18 km 48 × 54, 6 km 35 vertical levels
Domain centre	56.63° N, 3.35° W

meteorological conditions in northwest Europe, and therefore we expect a similar footprint. Henne et al. (2010) calculated a 12 h inversion, estimating the footprint of Mace Head to be the land surface within ~ 195 km of the tower. Therefore, if a similar footprint is assumed for TTA, ~ 98 % of the inner domain's land surface is within the footprint of TTA. We use this estimate of footprint to mask the area of the land surface that is presented throughout this study.

4 Results

4.1 CO₂ time series at TTA

We compared hourly observations of atmospheric CO₂ concentrations from TTA (2006–2008) with both the WRF-SPA simulated total atmospheric CO₂ ($R^2 = 0.67$, $rmse = 3.5$ ppm, $bias = 0.58$ ppm, linear regression) and “forcings only” CO₂ ($R^2 = 0.71$, $rmse = 3.3$ ppm, $bias = 0.82$ ppm). These results suggest a slightly negative impact of including the modelled biosphere. However, the annual bias for total atmospheric CO₂ from WRF-SPA is lower than “forcings only” CO₂, highlighting the impact of Scotland's biosphere sink (Fig. 2a). Furthermore, the addition of biospheric fluxes captures diurnal variation in hourly observations, which is otherwise absent in “forcings only” CO₂ (Fig. 2ab). However, inclusion of biospheric fluxes results in an overestimation of night-time atmospheric CO₂ concentrations simulated at the tall tower (Fig. 2b). A comparison between atmospheric CO₂ concentrations observed at TTA and the CTE (2006–2007) and CT (2008) atmospheric inversion model ($R^2 = 0.69$, $rmse = 3.5$ ppm, $bias = 0.92$ ppm) suggests comparable skill to WRF-SPA. However, CTE-CT does not simulate daily cycles in observed atmospheric CO₂ concentrations as well as WRF-SPA (Fig. 2b). As CTE-CT are available at 3-hourly intervals, the analysis was conducted against TTA observations averaged to a 3-hourly time step.

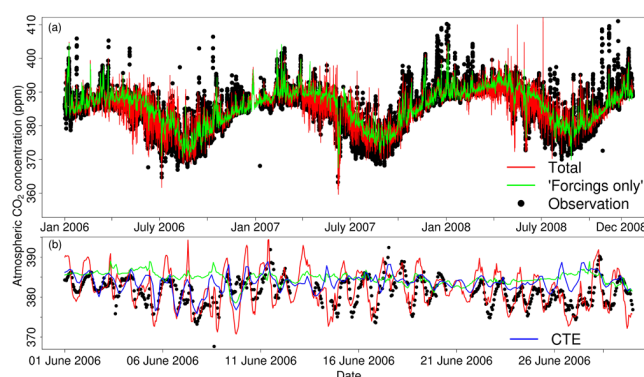


Fig. 2. Time series comparison between hourly observations of atmospheric CO₂ concentrations made at TTA and WRF-SPA simulated total atmospheric CO₂ and “forcings only” CO₂. Atmospheric CO₂ concentrations at 3-hourly time step from CTE-CT are also included in (b). (a) Shows that the simulated CO₂ time series (2006–2008) is mostly driven by forcings originating outside of the model domain, as indicated by “forcings only” CO₂. (b) Shows an hourly (3 hourly for CTE-CT) time series for June 2006, highlighting that diurnal variation in simulated CO₂ is due to exchange with the biosphere within the simulated domain, as total atmospheric CO₂ captures this variation. WRF-SPA modelled total atmospheric CO₂ contains all model forcings and exchange with the simulated biosphere, while “forcings only” CO₂ does not include biospheric exchange (i.e. total–biospheric fluxes comparison).

The impact of the biosphere is more clearly seen at seasonal timescales using monthly means (Fig. 3). Total atmospheric CO₂ ($R^2 = 0.96$, $rmse = 1.2$ ppm, $bias = 0.54$ ppm), which includes biospheric exchange, shows improved statistical agreement with observations compared to “forcings only” CO₂ ($R^2 = 0.91$, $rmse = 1.6$ ppm, $bias = 0.71$ ppm) and CTE-CT atmospheric CO₂ concentrations ($R^2 = 0.94$, $rmse = 1.5$ ppm, $bias = 0.94$ ppm). The monthly mean bias between total atmospheric CO₂ and observations is reduced for the majority of the comparison period relative to “forcings only” CO₂ and CTE-CT. The seasonal bias is reduced

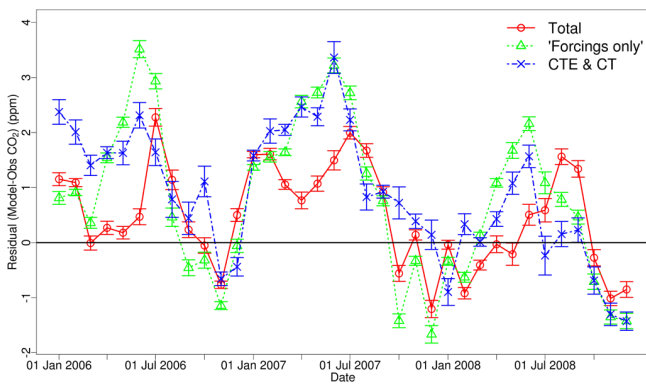


Fig. 3. Time series of monthly mean residual (Model-Obs) between observed, CTE-CT and WRF-SPA simulated total atmospheric CO₂ and “forcings only” concentrations. Highlights time periods during which the inclusion of the simulated biosphere results in a reduction in monthly mean bias. Error bars are ± 1 standard error, accounting for temporal and spatial uncertainty only.

in total atmospheric CO₂ by up to 2.8 ppm and 1.9 ppm between March and June of each year compared to “forcings only” CO₂ and CTE-CT, respectively (Fig. 3). However, the modelled biosphere does not capture the observed seasonal minimum in atmospheric CO₂ concentrations, which occurs in July–August of each year (Figs. 2 and 3). During July–September total atmospheric CO₂ has a larger bias than both “forcings only” CO₂ and CTE-CT compared to observations. A larger positive bias in total atmospheric CO₂ than “forcings only” CO₂ indicates that modelled ecosystems within the footprint of the tall tower have become a net source of CO₂ at a time when they should remain a net sink (Fig. 3).

4.2 Ecosystem contributions to atmospheric CO₂ concentrations at TTA

The dominant ecosystems simulated within the footprint are forest, crop and managed grassland (Fig. 1). Over the validation period WRF-SPA simulated forest ($-2.56 \pm 0.05 \text{ tC ha}^{-1} \text{ yr}^{-1}$, \pm standard error, accounting for spatial and temporal uncertainty only) and managed grassland ($-0.48 \pm 0.02 \text{ tC ha}^{-1} \text{ yr}^{-1}$) ecosystems to be mean annual sinks of carbon. Crop ecosystems ($0.89 \pm 0.01 \text{ tC ha}^{-1} \text{ yr}^{-1}$) were simulated to be a mean annual source of carbon. WRF-SPA estimates Scotland to be on average a carbon sink of $-0.99 \pm 0.04 \text{ tC ha}^{-1} \text{ yr}^{-1}$. CTE-CT estimates Scotland to be a carbon source of $+0.65 \text{ tC ha}^{-1} \text{ yr}^{-1}$.

Net uptake and net release CO₂ tracers simulated at TTA suggest that cropland ecosystems have a distinct seasonal cycle from that of forests, managed grassland and “other” land cover types (Fig. 4). Managed grassland and “other” land covers are not included in the figure due to their contribution to atmospheric CO₂ concentrations being small, never exceeding 0.7 ppm. Peak net uptake CO₂ tracer simulated

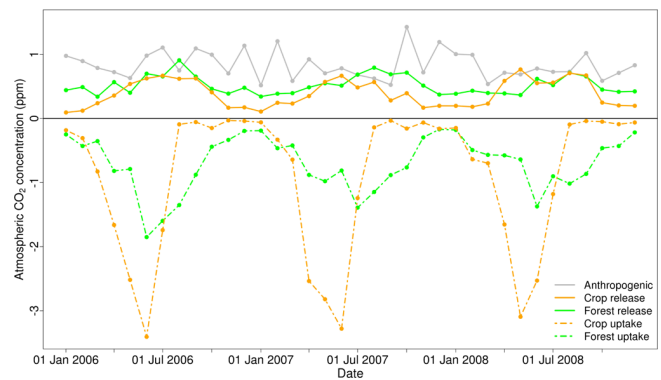


Fig. 4. Monthly mean mixing ratios for net uptake and net release CO₂ tracers for crop and forest ecosystems simulated at TTA. Highlights differences in detection of ecosystem processes at TTA, in particular the distinct seasonal cycle of cropland net uptake and net release CO₂ tracers compared to all other ecosystems. Managed grassland and “other” ecosystems are not included due to their small magnitude contributions, never exceeding 0.7 ppm.

at TTA occurs 1 month earlier in crops than forest (except in 2006), while net release CO₂ tracer simulated at TTA for cropland shows a similar seasonality to all other ecosystems. Peak crop respiration coincides with crop harvest, a point in time when plant biomass has undergone senescence and has subsequently either been removed as part of harvest processes or remains after harvest as residue added to the litter pool (mean simulated harvest day of year: 2006 is 225 ± 17.9 , 2007 is 229 ± 21.4 , 2008 is 229 ± 21.5 , standard deviation accounting for spatial variability only). While crops contribute a similar amount of net release CO₂ tracer as forest during the growing season, during winter crop net release CO₂ tracer is less than half that of forest (Fig. 4). Anthropogenic CO₂ simulated at TTA is comparable in magnitude to that of CO₂ released by the biosphere. Also, anthropogenic CO₂ does not display a strong seasonal trend (Fig. 4).

Forest and crops dominate the net uptake CO₂ tracer simulated at TTA (65–93 % of TTA tracer concentration and 72–91 % of surface flux) (Fig. 5). On average, crop and managed grassland are over-represented in net uptake CO₂ tracers simulated at TTA by 3 % and 3.4 %, respectively. Managed grassland represents on average just ~ 13 % of surface net CO₂ uptake flux compared to ~ 40 % for crops. Forest and “other” ecosystems are under-represented by 5 % and 1.2 %, respectively. However, the over/under-representation varies at seasonal timescales, e.g. the largest under-representation of forests at TTA occurs between August 2006 and January 2007 (21 %) while at other times atmospheric CO₂ simulated at TTA is more representative. The bias towards crops is consistent with the spatial distribution of crops and forest cover in relation to TTA’s location (Fig. 1). Crops is the dominant ecosystem, both in terms of net uptake CO₂ tracer and surface net CO₂ uptake flux during the growing season

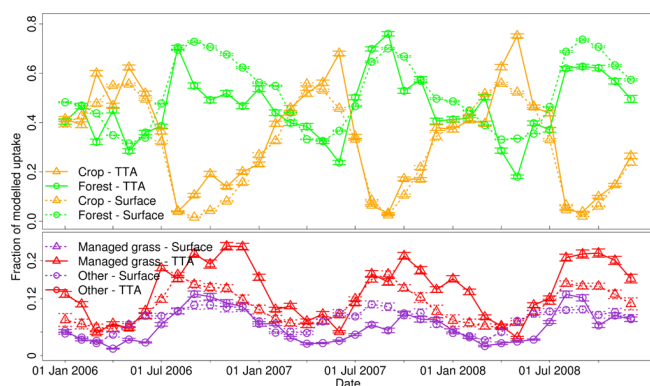


Fig. 5. Comparison between monthly mean ecosystem-specific fraction of net uptake CO₂ tracers simulated at TTA and fraction of surface net CO₂ uptake flux. Were an ecosystems fraction of net uptake CO₂ tracer to be greater than the corresponding fraction of surface net CO₂ uptake flux, it would indicate that the ecosystem is over-represented in total atmospheric CO₂ concentrations. The reverse would indicate that the ecosystem was under-represented. Error bars are ± 1 standard error, accounting for temporal and spatial uncertainty only.

(Fig. 5). After harvest (July of each year), forest becomes the dominant land cover for driving CO₂ exchange, as crop surface net CO₂ uptake flux declines due to senescence and removal of plants.

4.3 Seasonal and interannual variation

Net uptake CO₂ tracers simulated at TTA are able to explain the majority of seasonal variation in surface net CO₂ uptake for crops, forest, managed grassland and “other” land covers (Table 3). The seasonal cycles in net uptake CO₂ tracers are more variable during the growing season (i.e. May–August), such that there is a mismatch between peak net uptake CO₂ tracers and surface net CO₂ uptake flux by \pm one month (Fig. 6). Moreover, the amount of variation in surface net CO₂ flux explained by net uptake CO₂ tracers simulated at TTA varied between years (e.g. forest 2006 $R^2 = 0.79$ and 2008 $R^2 = 0.58$). The rank order of net uptake CO₂ tracers simulated at TTA from each year does not correspond with the rank order of surface net CO₂ uptake flux for any ecosystem (Fig. 6). Interannual variation in mean annual surface net CO₂ uptake flux was $\sim 9\%$ while interannual variation for mean annual net uptake CO₂ tracer at TTA was $\sim 19\%$.

The annual prevailing wind direction over Scotland varied between years; in 2006 and 2008 the prevailing wind direction was broadly south/southwest, while in 2007 the prevailing wind direction was westerly. Moreover, the prevailing wind direction varied at seasonal timescales. During the peak growing season (May to August) there was considerable variation (Fig. 7). In 2006 prevailing wind direction during the growing season varied between southerly and westerly. In 2007 and 2008 there were periods of northerly and

Table 3. Summary of R^2 values from regression analysis of variation in surface net CO₂ uptake flux explained by tall tower detected net CO₂ uptake tracers. A combined 2006 to 2008 period is provided to give an indication of overall performance, while individual years allow for consideration of interannual variation in detection capability.

	Crop	Forest	Managed grassland	“Other”
2006–2008	0.94	0.72	0.72	0.77
2006	0.94	0.76	0.82	0.85
2007	0.94	0.74	0.58	0.71
2008	0.96	0.58	0.69	0.70

easterly winds, particularly during June; returning to more southwesterly directions by August in each year. This interannual and seasonal variation in wind direction would likely have impacted the detected footprint by TTA.

5 Discussion

5.1 CO₂ time series

WRF-SPA demonstrated that it can recreate observations of atmospheric CO₂ concentrations (Fig. 2a and b). The dominant seasonal cycle reproduced by WRF-SPA is largely driven by forcings external to the modelled domain, i.e. the global signal from lateral boundary conditions (Fig. 2a), as indicated by the “forcings only” CO₂ tracer. Atmospheric CO₂ concentrations are underestimated during the winter; however, the bias is of a smaller magnitude in total atmospheric CO₂ than in “forcings only” CO₂ (Fig. 3). The underestimation during winter likely indicates that SPA underestimates net release of CO₂ flux (i.e. respiration) from the land surface. WRF-SPA has previously been validated against eddy covariance observations of NEE at forest, managed grassland and cropland sites, where forest and managed grassland NEE was overestimated during winter while cropland was underestimated (Smallman et al., 2013). Given that net release CO₂ tracers simulated at TTA for crops is half the magnitude for forests, crops are a plausible candidate to explain the wintertime underestimate in simulated atmospheric CO₂ concentrations (Fig. 4). Smallman et al. (2013) hypothesised that the underestimate in crop could be related to an underestimation of soil organic matter or the rate of soil organic matter turnover within the carbon model; however, there remain several possibilities to be explored (e.g. ploughing).

In contrast, CTE-CT continues to overestimate atmospheric CO₂ until late in the year (November/December), indicating that the inversion analysis continues to underestimate Scotland’s carbon sink/overestimate carbon source during this period (Fig. 3). The WRF-SPA modelled biosphere generates diurnal cycles of realistic magnitude in the

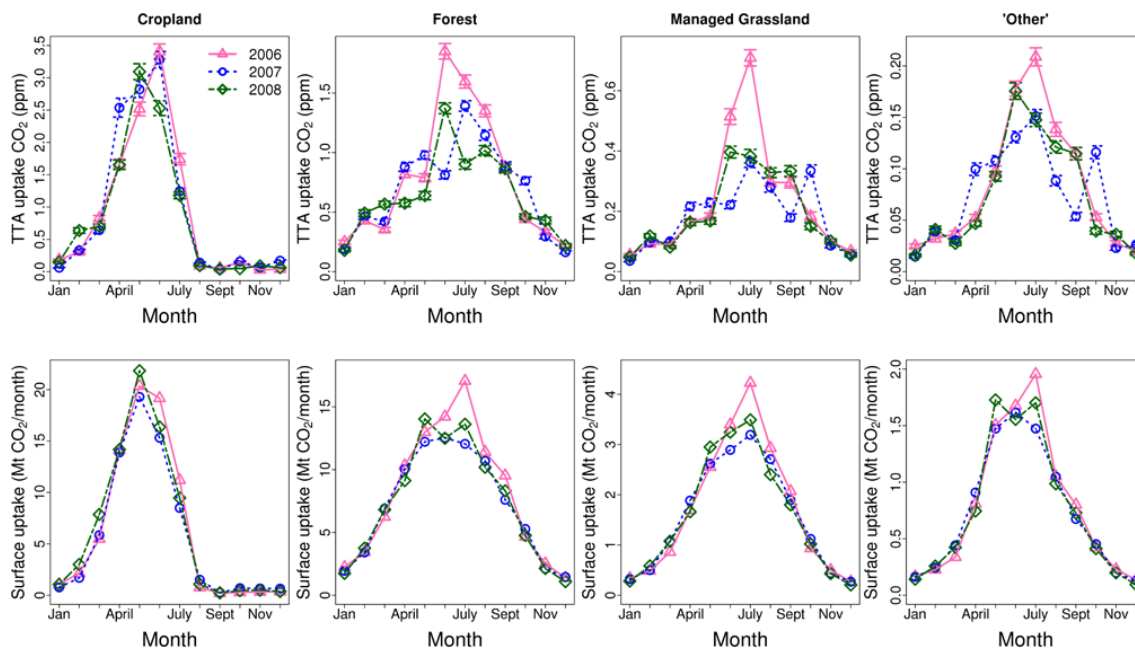


Fig. 6. Seasonal and interannual comparison between monthly mean net uptake CO₂ tracer simulated at TTA for crop, forest, managed grassland and “other” (upper panels), and monthly sum surface net CO₂ uptake flux (lower panels). Note the different scales between ecosystem types. Error bars are ±1 standard error, accounting for temporal and spatial uncertainty only.

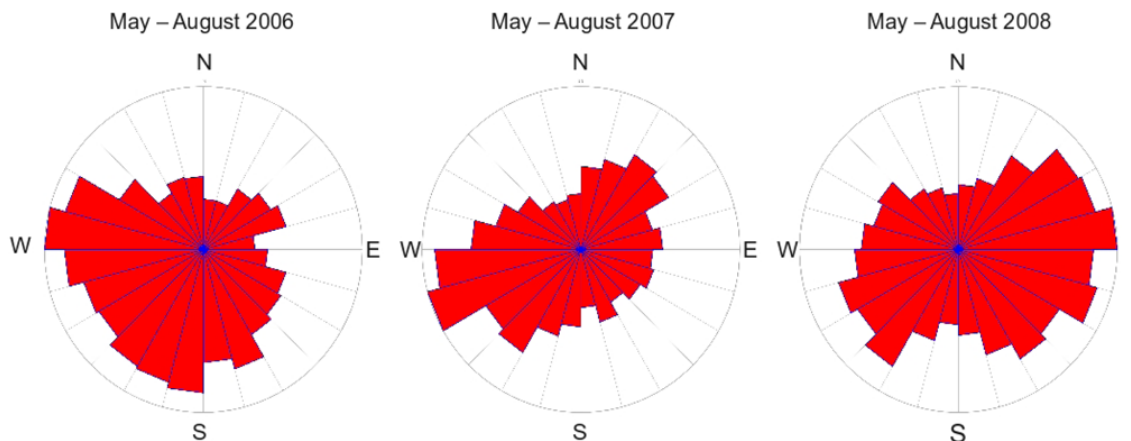


Fig. 7. Interannual comparison of growing season (May, June, July and August) prevailing wind direction at TTA. The wind rose shows the count of hourly wind directions simulated by WRF-SPA, where the direction indicated is the direction from which the wind is coming.

modelled CO₂ time series (Fig. 2b) and reduces the seasonal bias seen in “forcing only” CO₂ (Fig. 3); however, nocturnal atmospheric CO₂ concentrations are overestimated. The nocturnal overestimation of atmospheric CO₂ concentrations is likely due to an error in the YSU PBL scheme used in WRF-SPA. The error results in an overestimation of atmospheric eddy diffusivity under stable conditions, ultimately leading to a higher PBL (Hu et al., 2013). However, given that daytime CO₂ concentrations remain well simulated, it is unlikely that the nocturnal error persists into the well-mixed boundary layer due to rapid turnover of the atmosphere through

nudging by LBCs. Moreover, WRF-SPA has been previously assessed against surface fluxes of heat, water and CO₂, and daytime vertical profiles of atmospheric CO₂ concentrations where profile structure was well simulated, from which we can infer appropriate atmospheric transport (Smallman et al., 2013). Furthermore, WRF-SPA’s performance is comparable to several studies that have compared observations of atmospheric CO₂ concentrations made at tall towers to high resolution mesoscale model simulations (e.g. Ahmadov et al., 2009; Tolk et al., 2009; Pillai et al., 2011).

Atmospheric CO₂ concentrations from CTE-CT were also compared to observation made at TTA, at both 3-hourly averaged (Fig. 2b) and monthly mean timescales (Fig. 3). The statistical comparison suggests little impact of high resolution simulation using WRF-SPA, which contrasts with similar comparisons between high and coarse horizontal resolution models (e.g. Ahmadov et al., 2009). However, CTE-CT did not capture the observed diurnal cycle seen in TTA observations as well as WRF-SPA (Fig. 2b). The mean bias between observations of atmospheric CO₂ concentrations from TTA (which are not included in the CTE-CT atmospheric inversion) and CTE-CT is comparable to towers which were included in the inverse model (Peters et al., 2010). At seasonal timescales, CTE-CT tends to show a reduced bias compared with “forcings only” CO₂; however, the growing season bias remains larger than in total atmospheric CO₂ concentrations simulated by WRF-SPA (Fig. 3).

The prevailing wind direction over the UK is southwesterly, allowing the tower at Mace Head, Ireland, to provide an estimate of the background CO₂ concentration and to act as a boundary condition upwind of the air which passes over Scotland. Mace Head is used to provide a boundary condition in the CTE-CT atmospheric inversion (Peters et al., 2010). Importantly, the bias between observations made at Mace Head and CTE-CT is small at +0.05 ppm (Peters et al., 2010). Therefore, it can be inferred that the errors between modelled estimates of atmospheric CO₂ concentrations and observations is largely due to the simulation of surface exchanges within the model domain presented here.

5.2 Scotland's carbon balance

WRF-SPA's estimate of carbon sink magnitude is ~5 fold greater than the official estimate of Scotland's carbon sink by the UK National Atmospheric Emissions Inventory (NAEI), which estimates Scotland's carbon balance, for CO₂, to be $-0.20 \text{ tC ha}^{-1} \text{ yr}^{-1}$ (Thomson et al., 2012). WRF-SPA does not account for a number of management impacts, such as biomass burning and land cover change. Excluding these fluxes, the NAEI estimate for Scotland's carbon sink is $-0.44 \text{ tC ha}^{-1} \text{ yr}^{-1}$. While WRF-SPA agrees with the NAEI that Scotland is a net sink of carbon, there appears to be a large discrepancy in the magnitude of the sink strength, the causes of which remain to be identified. However, as we currently lack an error analysis of atmospheric CO₂ concentrations simulated by WRF-SPA, it remains unknown whether the discrepancy shown here is within errors.

WRF-SPA simulated mean forest sequestration ($-2.56 \text{ tC ha}^{-1} \text{ yr}^{-1}$) is approximately double the estimates for UK wide (Cannell et al., 1999) and average European forest sequestration (Janssens et al., 2005; Luyssaert et al., 2010). Scotland-specific estimates of forest sequestration are more similar to the simulations; Scotland-specific estimates range between $\sim 1.8 \text{ tC ha}^{-1} \text{ yr}^{-1}$ (Thomson et al., 2012) and $\sim 2.0 \text{ tC ha}^{-1} \text{ yr}^{-1}$ (Forestry Commission Scotland,

2009). Forest activity is under-represented in atmospheric CO₂ concentrations simulated at TTA, as indicated by the lower fraction of net uptake CO₂ tracer simulated at TTA compared to the fraction of surface net CO₂ uptake flux originating from forest land cover. This under-representation of forest cover may explain why there is no apparent over-estimation of Scotland's net carbon sink in the comparison between simulated CO₂ at TTA and observations. Grasslands were simulated to be a net carbon sink ($-0.48 \text{ tC ha}^{-1} \text{ yr}^{-1}$) while croplands were simulated to be a net carbon source ($0.89 \text{ tC ha}^{-1} \text{ yr}^{-1}$). Estimates of grassland carbon sink are more comparable with other estimates, which range between $-0.69 \text{ tC ha}^{-1} \text{ yr}^{-1}$ (UK average, Janssens et al., 2005) and $-0.15 \text{ tC ha}^{-1} \text{ yr}^{-1}$ (Scotland specific, Thomson et al., 2012). The WRF-SPA estimate of cropland source magnitude is also comparable with other UK wide ($0.53 \text{ tC ha}^{-1} \text{ yr}^{-1}$, Janssens et al., 2005) and Scotland-specific estimates ($0.88 \text{ tC ha}^{-1} \text{ yr}^{-1}$, Thomson et al., 2012).

The simulated representation of arable cropland within WRF-SPA is likely to be responsible for the increase in the monthly mean bias between July–September in total atmospheric CO₂ (Fig. 3). Cropland net uptake CO₂ tracer simulated at TTA declines in magnitude concurrently with the increase in total atmospheric CO₂ bias in July (Figs. 3 and 4). In addition, the total atmospheric CO₂ bias exceeds the “forcings only” CO₂ bias in August as cropland respiration increases due to the input of litter from harvest. Above-ground carbon is removed as part of the harvest, leaving a fraction of above-ground carbon as surface residue and root carbon within the soil. Both the surface residue and root carbon are added to the litter carbon pool, which begin to decompose significantly increasing respiration from cropland.

In Scotland, on average ~36% of agricultural land is uncultivated, including woodland patches, hedgerows and fallow land (Scottish Government, 2012). However, WRF-SPA does not simulate uncultivated land associated with agriculture. These nonmodelled vegetative components are likely to be perennial systems, lack intensive management and as a result have a longer growing season. For example, forest and managed grassland ecosystems continue to have a significant level of surface CO₂ uptake flux for several months after cropland harvest (Fig. 6). Therefore, uncultivated systems represent a significant contribution to the agricultural carbon balance at regional scales (Smith, 2004). Further development in the representation of agricultural land within LSMs is needed. For example, modelling at high spatial resolutions may allow land cover maps to resolve some of this heterogeneity; alternatively, a tiling system could be used to represent this sub-grid heterogeneity.

5.3 Representativeness and seasonal variation of TTA observations

Cropland is most often the dominant ecosystem-specific net uptake CO₂ tracer simulated at TTA and the dominant

surface net CO₂ uptake flux (Fig. 6). Cropland is also fractionally over-represented at TTA compared to its surface net CO₂ uptake flux (Fig. 5). Over-representation of crops is expected given the spatial distribution of the land cover types in relation to TTA (Fig. 1). Our results are consistent with other findings of both modelling and observational studies in this regard (Gerbig et al., 2009; Vermeulen et al., 2011; Lauvaux et al., 2012; Miles et al., 2012). Forests dominate the fractional activity after cropland harvest due to their continuing biological activity in the late summer (Figs. 5 and 6).

Atmospheric CO₂ concentrations simulated at TTA contains significant seasonal information on ecosystems that are not adjacent to the tower (i.e. forest, managed grassland and “other”). Forest dominance of the fraction of net uptake CO₂ tracer (Fig. 5) at TTA coincides with crop senescence and harvest (Fig. 4). The relatively small mismatches shown here seem likely to be explained by seasonal variation in tower footprint, as indicated by seasonal and interannual variation in prevailing wind direction (Fig. 7). Cropland is best represented by net uptake CO₂ flux tracers (Table 3), which is expected given the local dominance already discussed.

5.4 Interannual variation

Interannual variation of the simulated seasonal cycles in surface net CO₂ uptake flux is poorly represented by net uptake CO₂ tracers simulated at TTA (Fig. 6). Interannual variation of net uptake CO₂ tracers simulated at TTA is greater than interannual variation in modelled land surface net CO₂ uptake flux. This suggests that interannual variation in atmospheric transport due to year-to-year variation in weather, not variation in land surface net CO₂ uptake, is the dominant driver of interannual variation in tall tower observations for the years simulated here. This inference is supported by the interannual variation in wind direction, for example during the growing season (May, June, July and August) in 2008 where there is a larger incidence of easterly winds altering the observation footprint of TTA (Fig. 7). This highlights the need for careful attention to atmospheric transport uncertainties and errors when carrying out atmospheric inversions. To detect a change in land surface activity, the magnitude of the change must be greater than the variation in detection due to transport. Alternatively, an extended network of tall towers is required to gain spatially explicit information on land surface exchange (Lauvaux et al., 2012).

Net uptake CO₂ tracer concentrations for managed grassland and “other” land covers simulated at TTA are less than 0.7 ppm and 0.2 ppm, respectively. The accuracy limit for CO₂ detection of the equipment installed at TTA is 0.1 ppm. This suggests that limited real world information is present in TTA observations for managed grassland and “other” land covers in the MODIS map. Therefore, it is also likely that TTA provides limited information in the real world for any ecosystem with limited activity or small spatial extent. Ineffective detection of “other” vegetation is significant as

“other” land cover types include Scotland’s uplands and peatland areas. Upland and peatland areas are highly important given the significant amount of carbon stored as soil organic matter in these soils, estimated to contain > 200 tC ha⁻¹ (Bradley et al., 2005). However, it should be noted that the MODIS land cover map used in WRF-SPA does contain errors; the upland and peatland cover for Scotland in the MODIS map is ~ 3 % while more detailed mapping efforts of Scotland have estimated uplands and peatlands to cover a larger area (~ 17 % Macaulay Land Use Research Institute, 1993).

5.5 Future work

WRF-SPA estimates for ecosystem-specific mean annual sequestration are broadly reasonable; however, they should be considered with caution. This study does not estimate the SPA parameter uncertainties or uncertainties associated with atmospheric transport that may have a significant impact on the interpretation of sequestration estimates given here. As a result, estimates of ecosystem mean annual carbon sequestration should be considered only as indicators of consistency with other estimates. Therefore, future work should involve an appropriate data-driven uncertainty analysis of SPA parameters (i.e. data assimilation) and an attempt to assess atmospheric transport uncertainties.

WRF-SPA does not currently include a representation of forest management. Forest ecosystems are initialised with identical conditions that have been “spun up” into steady state. As a result, important differences in forest sequestration due to age class distribution and lateral transport of carbon due to forest harvest are not included. In future, a more detailed representation of forest processes should be included.

It remains to be investigated whether policy-relevant land cover management can be detected at TTA (e.g. afforestation). WRF-SPA simulations presented here indicate that observations made at TTA are unable to reliably detect interannual variation of ecosystems. However, tall towers are expected to be used for monitoring the effects of land surface management aimed at mitigating climate change (ICOS, 2012). Current Scottish government policy is to increase Scotland’s forest cover by 650 000 ha by 2050 (Forestry Commission Scotland, 2009). Through WRF-SPA the capability of current observations to detect changes in Scotland’s regional carbon balance should be investigated.

6 Conclusions

Three specific questions were asked of WRF-SPA to investigate atmospheric observations of CO₂ made mostly within the PBL from TTA, Scotland.

(i) Does WRF-SPA more accurately simulated observed atmospheric CO₂ concentrations compared to a coarse resolution global atmospheric inversion model? WRF-SPA does more accurately simulate observed atmospheric CO₂ concentrations at TTA compared to CTE-CT. WRF-SPA better represents diurnal variation and a reduced bias between simulated atmospheric CO₂ concentrations and observations, particularly during the growing season. (ii) Can ecosystem-specific CO₂ tracers be used to inform on which ecosystem processes and land covers are responsible for observed variations in atmospheric CO₂ concentrations? Ecosystem specific tracers have been successfully used to infer crops as being responsible for a increase in the bias between WRF-SPA simulated atmospheric CO₂ concentrations at observations post-harvest each year. Furthermore, we have hypothesised that the cause of the error is the lack of a representation of uncultivated components of agricultural land not currently parameterised for in WRF-SPA. (iii) Can observations made at TTA detect variation in ecosystem carbon uptake, for ecosystems within the footprint of TTA, at seasonal and interannual timescales? A majority of seasonal variation in surface net CO₂ uptake flux is explained by net uptake CO₂ tracers for each ecosystem. However, the amount of variation explained varied considerably between years. Moreover, interannual variation was not well captured, potentially due to seasonal and inter annual variation in the prevailing wind direction. However, for all other ecosystems interannual variation in atmospheric transport due to year-to-year variation in weather had a greater impact on tall tower observations than interannual variation in surface uptake.

Acknowledgements. The authors would like to thank the PhD project funding body, National Centre for Earth Observation, a Natural Environment Research Council research centre. Tall tower Angus has been funded since 2004 by EU FP5, FP6 grants.

Edited by: T. Laurila

References

- Ahmadov, R., Gerbig, C., Kretschmer, R., Körner, S., Rödenbeck, C., Bousquet, P., and Ramonet, M.: Comparing high resolution WRF-VPRM simulations and two global CO₂ transport models with coastal tower measurements of CO₂, *Biogeosciences*, 6, 807–817, doi:10.5194/bg-6-807-2009, 2009.
- Bradley, R., Milne, R., Bell, J., Lilly, A., Jordan, C., and Higgins, A.: A soil carbon and land use database for the United Kingdom, *Soil Use Manage.*, 21, 363–369, doi:10.1079/SUM2005351, 2005.
- Brunner, D., Henne, S., Keller, C. A., Reimann, S., Vollmer, M. K., O'Doherty, S., and Maione, M.: An extended Kalman-filter for regional scale inverse emission estimation, *Atmos. Chem. Phys.*, 12, 3455–3478, doi:10.5194/acp-12-3455-2012, 2012.
- Canadell, J. G., Le Quere, C., Raupach, M. R., Field, C. B., Buitenhuis, E. T., Ciais, P., Conway, T. J., Gillett, N. P., Houghton, R. A., and Marland, G.: Contributions to accelerating atmospheric CO₂ growth from economic activity, carbon intensity, and efficiency of natural sinks, *P. Natl. Acad. Sci. USA.*, 104, 18866–18870, doi:10.1073/pnas.0702737104, 2007.
- Cannell, M., Milne, R., Hargreaves, K., Brown, T., Cruickshank, M., Bradley, R., Spencer, T., Hope, D., Billett, M., Adger, W., and Subak, S.: National inventories of terrestrial carbon sources and sinks: The UK experience, *Climatic Change*, 42, 505–530, doi:10.1023/A:1005425807434, 1999.
- Ciais, P., Reichstein, M., Viovy, N., Granier, A., Ogee, J., Allard, V., Aubinet, M., Buchmann, N., Bernhofer, C., Carrara, A., Chevallier, F., De Noblet, N., Friend, A., Friedlingstein, P., Grunwald, T., Heinesch, B., Keronen, P., Knohl, A., Krinner, G., Loustau, D., Manca, G., Matteucci, G., Miglietta, F., Ourcival, J., Papale, D., Pilegaard, K., Rambal, S., Seufert, G., Soussana, J., Sanz, M., Schulze, E., Vesala, T., and Valentini, R.: Europe-wide reduction in primary productivity caused by the heat and drought in 2003, *Nature*, 437, 529–533, 2005.
- Farquhar, G. D. and von Caemmerer, S.: Modelling of photosynthetic response to the environment, *Physiological Plant Ecology II. Encyclopedia of plant physiology*, Springer-Verlag, Berlin, 1982.
- Forestry Commission Scotland: The Scottish Government's Rational for Woodland Expansion, The scottish government strategy document, Forestry Commission, Edinburgh, EH12 7AT, Scotland, 2009.
- Gerbig, C., Dolman, A. J., and Heimann, M.: On observational and modelling strategies targeted at regional carbon exchange over continents, *Biogeosciences*, 6, 1949–1959, doi:10.5194/bg-6-1949-2009, 2009.
- Gurney, K., Law, R., Denning, A., Rayner, P., Baker, D., Bousquet, P., Bruhwiler, L., Chen, Y., Ciais, P., Fan, S., Fung, I., Gloor, M., Heimann, M., Higuchi, K., John, J., Maki, T., Maksyutov, S., Masarie, K., Peylin, P., Prather, M., Pak, B., Randerson, J., Sarmiento, J., Taguchi, S., Takahashi, T., and Yuen, C.: Towards robust regional estimates of CO₂ sources and sinks using atmospheric transport models, *Nature*, 415, 626–630, doi:10.1038/415626a, 2002.
- Henne, S., Brunner, D., Folini, D., Solberg, S., Klausen, J., and Buchmann, B.: Assessment of parameters describing representativeness of air quality in-situ measurement sites, *Atmos. Chem. Phys.*, 10, 3561–3581, doi:10.5194/acp-10-3561-2010, 2010.
- Hu, X.-M., Klein, P. M., and Xue, M.: Evaluation of the updated YSU planetary boundary layer scheme within WRF for wind resource and air quality assessments, *J. Geophys. Res.-Atmos.*, 118, 1–16, doi:10.1002/jgrd.50823, 2013.
- ICOS: Integrated Carbon Observing System: Stakeholders Handbook, A European Infrastructure – European Union, LSCE-Orme, CEA-Orme des Merisiers, F-91191 GIF-SUR-YVETTE CEDEX, 2012.
- IPCC: Climate Change 2007: The Physical Basis. Contribution of Working Group I to the Fourth Assessment Report of the Intergovernmental Panel on Climate Change., edited by: Solomon, S., Qin, D., Manning, M., Chen, Z., Marquis, M., Averyt, K. B., Tignor, M., and Miller, H. L., Cambridge University Press, United Kingdom and New York, NY, USA, Cambridge, United Kingdom and New York, NY, USA, 2007.
- Janssens, I. A., Freibauer, A., Schlamadinger, B., Ceulemans, R., Ciais, P., Dolman, A. J., Heimann, M., Nabuurs, G.-J., Smith, P., Valentini, R., and Schulze, E.-D.: The carbon budget of terres-

- trial ecosystems at country-scale – a European case study, *Bio-geosciences*, 2, 15–26, doi:10.5194/bg-2-15-2005, 2005.
- Jones, H. G.: Plants and microclimate, Cambridge University Press, Cambridge, 1992.
- Lauvaux, T., Schuh, A. E., Bocquet, M., Wu, L., Richardson, S., Miles, N., and Davis, K. J.: Network design for mesoscale inversions of CO₂ sources and sinks, *Tellus Ser. B-Chem. Phys. Meteorol.*, 64, 17980, doi:10.3402/tellusb.v64i0.17980, 2012.
- Luyssaert, S., Ciais, P., Piao, S. L., Schulze, E. D., Jung, M., Zaehle, S., Schelhaas, M. J., Reichstein, M., Churkina, G., Papale, D., Abril, G., Beer, C., Grace, J., Loustau, D., Matteucci, G., Mag-nani, F., Nabuurs, G. J., Verbeeck, H., Sulkava, M., van der Werf, G. R., Janssens, I. A., and CARBOEUROPE-IP Synth Team: The European carbon balance. Part 3: forests, *Glob. Change Biol.*, 16, 1429–1450, doi:10.1111/j.1365-2486.2009.02056.x, 2010.
- Macaulay Land Use Research Institute: The land cover of Scot-land 1988: Executive Summary, The scottish government strat-egy document, The Macaulay Land Use Research Institute, Ab-erdeen, AB9 2QJ, Scotland, ISBN 0 7084 0538 X, 1993.
- Mesoscale and Microscale Meteorology Division: Weather Re-search and Forecasting ARW Version 3 Modelling System User's Guide, User's guide, National Center for Atmospheric Research, Colorado, USA, 2011.
- Miles, N. L., Richardson, S. J., Davis, K. J., Lauvaux, T., Andrews, A. E., West, T. O., Bandaru, V., and Crosson, E. R.: Large am-plitude spatial and temporal gradients in atmospheric boundary layer CO₂ mole fractions detected with a tower-based network in the U.S. upper Midwest, *J. Geophys. Res.-Biogeo.*, 117, G01019, doi:10.1029/2011JG001781, 2012.
- Peters, W., Jacobson, A. R., Sweeney, C., Andrews, A. E., Con-way, T. J., Masarie, K., Miller, J. B., Bruhwiler, L. M. P., Petron, G., Hirsch, A. I., Worthy, D. E. J., van der Werf, G. R., Ran-derston, J. T., Wennberg, P. O., Krol, M. C., and Tans, P. P.: An atmospheric perspective on North American carbon dioxide ex-change: CarbonTracker, *P. Natl. Acad. Sci. USA.*, 104, 18925–18930, 2007.
- Peters, W., Krol, M. C., van der Werf, G. R., Houweling, S., Jones, C. D., Hughes, J., Schaefer, K., Masarie, K. A., Jacobson, A. R., Miller, J. B., Cho, C. H., Ramonet, M., Schmidt, M., Ciattaglia, L., Apadula, F., Helta, D., Meinhardt, F., di Sarra, A. G., Pi-acentino, S., Sferlazzo, D., Aalto, T., Hatakka, J., Strom, J., Haszpra, L., Meijer, H. A. J., van der Laan, S., Neubert, R. E. M., Jordan, A., Rodo, X., Morgui, J. A., Vermeulen, A. T., Popa, E., Rozanski, K., Zimnoch, M., Manning, A. C., Leuen-berger, M., Uglietti, C., Dolman, A. J., Ciais, P., Heimann, M., and Tans, P. P.: Seven years of recent European net terrestrial carbon dioxide exchange constrained by atmospheric observa-tions, *Glob. Change Biol.*, 16, 1317–1337, doi:10.1111/j.1365-2486.2009.02078.x, 2010.
- Pillai, D., Gerbig, C., Ahmadvov, R., Rödenbeck, C., Kretschmer, R., Koch, T., Thompson, R., Neining, B., and Lavrié, J. V.: High-resolution simulations of atmospheric CO₂ over complex terrain – representing the Ochsenkopf mountain tall tower, *At-mos. Chem. Phys.*, 11, 7445–7464, doi:10.5194/acp-11-7445-2011, 2011.
- Rigby, M., Manning, A. J., and Prinn, R. G.: Inversion of long-lived trace gas emissions using combined Eulerian and Lagrangian chemical transport models, *Atmos. Chem. Phys.*, 11, 9887–9898, doi:10.5194/acp-11-9887-2011, 2011.
- Scottish Government: Scottish Agricultural Census, A national statistics publication for scotland: Agricultural series, The Scot-tish Government, 2012.
- Skamarock, W. C., Klemp, J. B., Dudhia, J., Gill, D. O., Barker, D. M., Duda, M. G., Huang, X.-Y., Wang, W., and Powers, J. G.: A Description of the Advanced research WRF Version 3, 2008.
- Smallman, T. L., Moncrieff, J. B., and Williams, M.: WRFv3.2-SPAv2: development and validation of a coupled ecosystem-atmosphere model, scaling from surface fluxes of CO₂ and en-ergy to atmospheric profiles, *Geosci. Model Dev.*, 6, 1079–1093, doi:10.5194/gmd-6-1079-2013, 2013.
- Smith, P.: Carbon sequestration in croplands: the potential in Europe and the global context, *Eur. J. Agron.*, 20, 229–236, doi:10.1016/j.eja.2003.08.002, 2004.
- Steenefeld, G. J., Tolck, L. F., Moene, A. F., Hartogensis, O. K., Peters, W., and Holtslag, A. A. M.: Confronting the WRF and RAMS mesoscale models with innovative observations in the Netherlands: Evaluating the boundary layer heat budget, *J. Geo-phys. Res.-Atmos.*, 116, D23114, doi:10.1029/2011JD016303, 2011.
- Sus, O., Williams, M., Bernhofer, C., Beziat, P., Buchmann, N., Ceschia, E., Doherty, R., Eugster, W., Gruenwald, T., Kutsch, W., Smith, P., and Wattenbach, M.: A linked carbon cycle and crop developmental model: Description and evaluation against measurements of carbon fluxes and carbon stocks at several Eu-ropean agricultural sites, *Agr. Ecosyst. Environ.*, 139, 402–418, 2010.
- Thomson, A. M., Hallsworth, S., and Malcolm, H.: Emissions and Removals of Greenhouse Gases from Land Use, Land Use Change and Forestry (LULUCF) for England, Scotland, Wales and Northern Ireland: 1990-2010, Department for Energy and Climate Change Contract GA0510, 2012.
- Tolk, L. F., Peters, W., Meesters, A. G. C. A., Groenendijk, M., Ver-meulen, A. T., Steenefeld, G. J., and Dolman, A. J.: Modelling regional scale surface fluxes, meteorology and CO₂ mixing ra-tios for the Cabauw tower in the Netherlands, *Biogeosciences*, 6, 2265–2280, doi:10.5194/bg-6-2265-2009, 2009.
- Vermeulen, A. T., Hensen, A., Popa, M. E., van den Bulk, W. C. M., and Jongejan, P. A. C.: Greenhouse gas observations from Cabauw Tall Tower (1992–2010), *Atmos. Meas. Tech.*, 4, 617–644, doi:10.5194/amt-4-617-2011, 2011.
- Williams, M., Rastetter, E. B., Fernandes, D. N., Goulden, M. L., Wofsy, S. C., Shaver, G. R., Melillo, J. M., Munger, J. W., Fan, S. M., and Nadelhoffer, K. J.: Modelling the soil-plant-atmosphere continuum in a Quercus-Acer stand at Harvard For-est: the regulation of stomatal conductance by light, nitrogen and soil/plant hydraulic properties, *Plant Cell Environ.*, 19, 911–927, 1996.
- Williams, M., Schwarz, P. A., Law, B. E., Irvine, J., and Kurpius, M.: An improved analysis of forest carbon dynamics using data assimilation, *Glob. Change Biol.*, 11, 89–105, 2005.
- Williams, M., Malhi, Y., Nobre, A., Rastetter, E., Grace, J., and Pereira, M.: Seasonal variation in net carbon exchange and evap-otranspiration in a Brazilian rain forest: a modelling analysis, *Plant Cell Environ.*, 21, 953–968, 1998.
- Williams, M., Law, B., Anthoni, P., and Unsworth, M.: Use of a simulation model and ecosystem flux data to examine carbon-water interactions in Ponderosa pine, *Tree Physiol.*, 21, 287–298, 2001.